Spectrum of Engineering Sciences
ISSN (e) 3007-3138 (p) 3007-312X Volume 3, Issue 7, 2025

DESIGN AND DEVELOPMENT OF MULTIFUNCTIONAL METASURFACE FOR BEAM STEERING AND POLARIZATION CONVERSION

Syed Elliyeen Shah[1], Muhammad Bilal[2], Muhammad Usman[3], Bilal Ur Rehman[4*], Kifayat Ullah[5], Muhammad Amir[6], Shahid Bashir[7], Muhammad Iftikhar[8]

[1,2,3,*4,5,6,7,8]*Department of Electrical Engineering, University of Engineering and Technology, Peshawar, Pakistan*

DOI: https://doi.org/ 10.5281/zenodo.16436186

Keywords
Metasurface, Beam Steering, Polarization.

Article History
Received: 26 April, 2025
Accepted: 11 July, 2025
Published: 26 July, 2025

Corresponding Author: *
Bilal Ur Rehman

Abstract *This study investigates the design and modelling of a multifunctional metasurface for polarization conversion, optimised with CST Microwave Studio. The metasurface, characterised by a C-shaped unit cell, attains a high polarization conversion efficiency (PCR > 90%) in the C-, X-, Ku-, and K-bands, exhibiting superior performance in the 5.3-5.4 GHz, 7.6-8.5 GHz, and 12.7-14.2 GHz frequency ranges. The research further introduces a broadband reflecting metasurface configuration that exhibits directional scattering characteristics and extensive phase tunability, operating across the 90-300 GHz range. Simulations indicate a phase shift range of +30° to -850 ° and exhibit pronounced directed reflection with reduced side lobes in bistatic radar cross-section (RCS) patterns. These findings highlight the metasurface's applications in advanced communication systems, beamforming, and stealth technologies.*

.

INTRODUCTION

The evolution of wireless communication technologies, including 5G networks, satellite communications, autonomous vehicle systems, and the Internet of Things (IoT), has increased the demanding nature of antenna systems and the need to generate higher throughput, lower latency, small size, less power usage, and the ability to work in numerous environments. The standard antenna designs do not always satisfy these requirements, especially concerning beam steering and polarization flexibility [1]. Mechanical motion or phased array are traditional beam steering techniques, which are usually large, power-hungry, and expensive. Polarization inconsistencies between transmitting and receiving antennas lead to low signal levels, poor data rates, and poor system performance. Error polarization remains a significant issue in several wireless communication systems, including 5G and satellite communication, where polarization alignment plays a crucial role in ensuring reliable signal reception and delivery [2]. To address them, an alternative is the concept of metasurfaces patented by the Lee Lab, which are engineered, planar materials with subwavelength unit cells (also known as meta-atoms). Unlike

traditional materials, metasurfaces can highly manipulate electromagnetic (EM) waves at the amplitude, phase and polarization levels. Their two-dimensional design has several advantages over three-dimensional metamaterials, including being smaller, lighter, and cheaper to manufacture [3]. Moreover, some of the various possibilities of metasurfaces include beam steering and polarization conversion, and they require no mechanical components or complex electronics. They, therefore, make them the best in small, high-efficiency antennas applicable in next-generation wireless installations [4]. One of the significant benefits of metasurfaces is the ability to present multifunctional capabilities in a single platform. By precisely controlling and arranging the meta-atoms, the waves can have their overall propagation directions altered dynamically using metasurfaces, thus allowing them to act as source-steerable electronic beams and providing a significant enhancement in the performance of communication systems. Thus, it enables the effective and reliable conduction of signals without the need for bulky mechanical parts [5]. In addition, metasurfaces can perform polarization conversion, converting incident waves to other polarization states as necessary. In some communication systems, mostly linear polarization is used, and care must be taken to ensure that polarization is set the same between the transmitter and the receiver to reduce the polarization mismatch loss and increase signal reception [6]. Metasurfaces are both functional, economical, and scalable, and they can be fabricated in large quantities using conventional fabrication processes such as photolithography, inkjet printing, and nanoimprinting [7].

Furthermore, a metasurface may include programmable elements, such as varactors, PIN diodes, or MEMS, allowing for the dynamic alteration of their electromagnetic behaviour [8]. This flexibility makes them highly versatile, allowing them to be adapted to support a wide range of operating conditions and align with the highly dynamic demands of modern wireless networks [9]. Metasurfaces have garnered significant attention for various applications, including radar systems, smart sensors, holography, wireless power transfer, and optical devices, due to their unique properties. Applicable to radar applications, metasurfaces can change the radar cross-section of objects or improve the detection and tracking of targets [10]. Satellite systems feature metasurface antennas, which can help save space on the payload, achieve high efficiency, and offer programmability [11]. In addition, metasurfaces are also under consideration as components of intelligent infrastructure, with applications in intelligent traffic management, specifically in the ability to alter the polarization of passed radar waves, thereby improving the pickup and discrimination of traffic signs amid wider interference [12]-[15].

This paper proposes and utilises a multifunctional lobed metasurface antenna design that incorporates beam steering and polarization conversion capabilities through a compact, adjustable structure. The proposed solution is to incorporate adjustable components into the metasurface layout, which dynamically changes the direction of the beam and the polarization state of an antenna, offering a versatile and responsive method of meeting current communication needs. Such a two-fold ability will significantly improve the performance, flexibility, and efficiency of wireless communication systems as a solid answer to the new enigma in antenna design. The growing demand for flexible regulation of electromagnetic wave propagation in modern wireless communication systems necessitates the development of sophisticated antenna technology. The classic designs of antennas face a problem when they need to control both the direction of the beam and its polarization at once, especially with reconfigurability and smaller antennas. As a solution, the manipulation of

wavefronts using metasurfaces offers the ability to control the wavefront perfectly in a practical, non-mechanical, and non-cumbersome manner. The focus of the study is to highlight the potential of metasurfaces in addressing some of the design challenges pertinent to the design and development of antennas, thereby enabling more efficient, wider applications, and scalable antenna solutions for next-generation communication technology.

2. LITERATURE REVIEW

Conventional systems that rely on mechanical movement or phased array structures face challenges in terms of dimension, energy, and cost [16]. Furthermore, the sending and receiving antennas need to be incompatible with each other, as the sending device will be significantly attenuated by having a very low data rate. The overall performance of the system will not be successful. The mismatches in polarization constitute a significant problem in wireless communication systems, where antennas are used to receive and transmit signals, such as in 5G and satellite communication connections, where the alignment of right polarization is essential for providing good reception and signal transfer [17]. The solution to such limitations is the use of metasurfaces, which are designed as planar materials with subwavelength unit cells, known as meta-atoms. Unlike traditional materials, metasurfaces enable complete control of electromagnetic (EM) waves in terms of amplitude, phase and polarization. The fact that they are two-dimensional has several advantages over three-dimensional metamaterials, including a decrease in size, weight, and lower manufacturing costs [18].

Additionally, metasurfaces can perform multiple operations, such as beam steering and polarization conversion, without the use of mechanical elements or a complicated electronic system. Those properties make them particularly suitable for use in wirelessly advanced systems, such as small high-performance antenna designs [19]. Metasurfaces possess a desirable property, namely the capability to support multifunctionality on a single platform. Meta-atoms enable metasurfaces to dynamically control the direction of wave propagation, offering electronic beam steering, and thereby enhancing the capabilities of communication systems. Hence, it enables reliable and effective transmission of signals without the need for bulky mechanical devices [20]. In addition, metasurfaces can also perform polarization conversion, making the incident waves transform into other polarization states as necessary. In various communication systems where linear polarization is deployed, it is crucial to ensure that there is polarization synchronization between the transmitting and receiving antennas to minimize polarization mismatch losses and maximize signal reception [21]. Metasurfaces are economically viable and scalable, allowing them to be produced in large quantities using regular fabrication processes, such as photolithography, inkjet printing, or nanoimprinting [22]. Reconfigurable components (varactors, PIN diodes or MEMS) may be integrated with the metasurfaces, facilitating the rapid switching of their electromagnetic response [23]. Metasurfaces enable a large number of operating states through reconfigurability, meeting the diverse needs of modern wireless systems [24]. Metasurfaces have been of great interest due to their unique properties, which have been utilized in radar systems, smart sensors, holography, wireless power transmission, and optical devices [25]. Metasurfaces in radar systems can modify the radar cross-section of objects or enhance target detection and tracking. Satellite antennas utilizing metasurfaces will be able to conserve payload volume while offering high operational efficiency and programmability [26]. Moreover, meta-surfaces are explored for use in smart infrastructure, such as intelligent traffic signs, which alter the polarization of bounced radar

signals, thereby enhancing detection and allowing it to be distinguished from incident noise [27].

The research suggests the development and invention of a multifunctional metasurface antenna that utilizes beam steering and polarization conversion capabilities within a compact and versatile structure. The currently proposed antenna could dynamically change direction and polarization state by adding adjustable capabilities to the metasurface design. The duality will deliver an effective yet multifaceted response to modern-day communication needs, promoting the enrichment, flexibility, and effectiveness of wireless communication systems. Moreover, the traditional antennas are facing limitations when handling the beam direction and polarization at the same time, especially in reconfigurable (and miniaturized) systems. The requirements set by the limits of resolution are best satisfied by meta-surfaces, which, due to their ability to modify electromagnetic wavefronts accurately, are capable of producing maximum wavefront curvatures in non-free spaces. The efficacy of modern communication systems, such as 5G and satellite communications, can be enhanced with the aid of meta-surfaces, which enable the dynamic control of wave propagation and surpass the limitations of traditional antenna technologies. The ability to phase, amplitude and polarization on a single platform, with no unwieldy components attached, makes metasurfaces a radical technology for small but high-performance antennas. The given research contributes to the existing body of knowledge by exploring how beam steering and polarization conversion may be incorporated into a unified metasurface design that meets the key requirements of modern wireless systems.

3. METHODOLOGY

The research employed a gradual simulation technique, consisting of various consecutive stages, to design, optimize, and evaluate the multifunctional metasurface. Analysis of the steering of polarised beams and the process of polarization conversion was conducted theoretically, initially determining key principles of the central design. A metasurface structure, with both unit cell and supercell topologies, was modelled using CST Microwave Studio. Appropriate material specifications and geometrical dimensions were outlined to ensure the compliance of the required frequency bands. The effects of variations in radius, breadth, length, and opening gap of a C-shaped resonator on the electromagnetic response were investigated through a thorough parametric sweep study. After design evaluation, full-wave simulations were conducted to obtain reflection coefficients, reflection phases, and polarization conversion ratios. The final step involved a comparative analysis of the performance of the reference metasurface with that of the optimized designs. Figure 1 illustrates the general methodological procedure, outlining all phases and explaining the step-by-step process from theoretical modelling to performance measurement and comparative analysis.

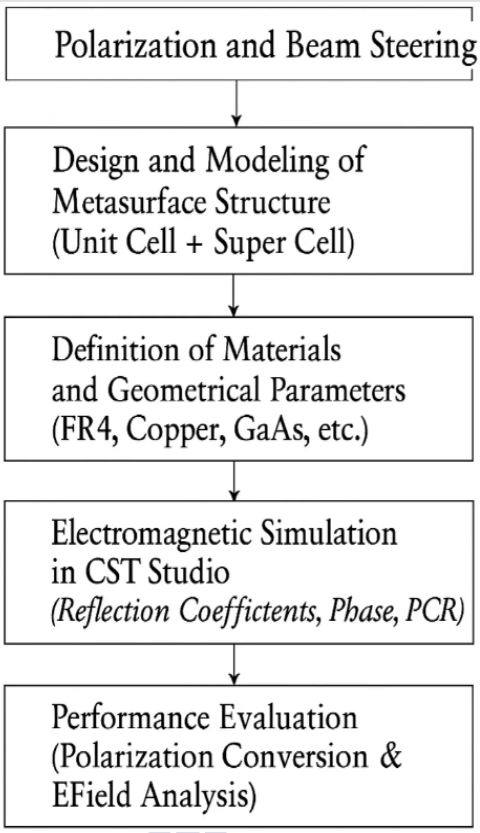

Figure 1: Flow diagram of proposed methodology.

A. Design and Modeling of the Metasurface

The metasurface is composed of a periodic array of C-shaped unit cells printed on an FR4 dielectric substrate backed by a metallic ground planeto operate in reflection mode as shown in Figure 2. The structure was chosen for its simplicity, compactness, and potential to generate both magnetic and electric resonances.

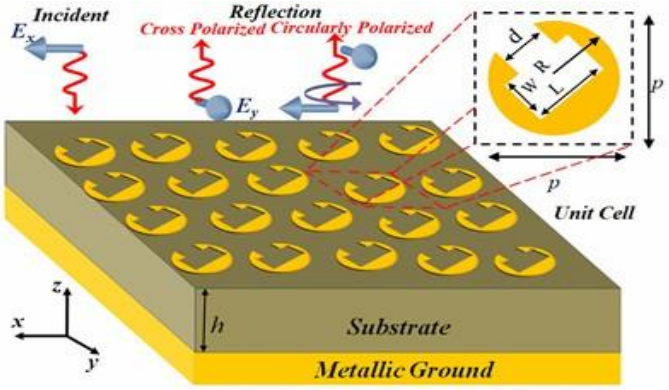

Figure 2: Schematic view of the metasurface and unit cell design

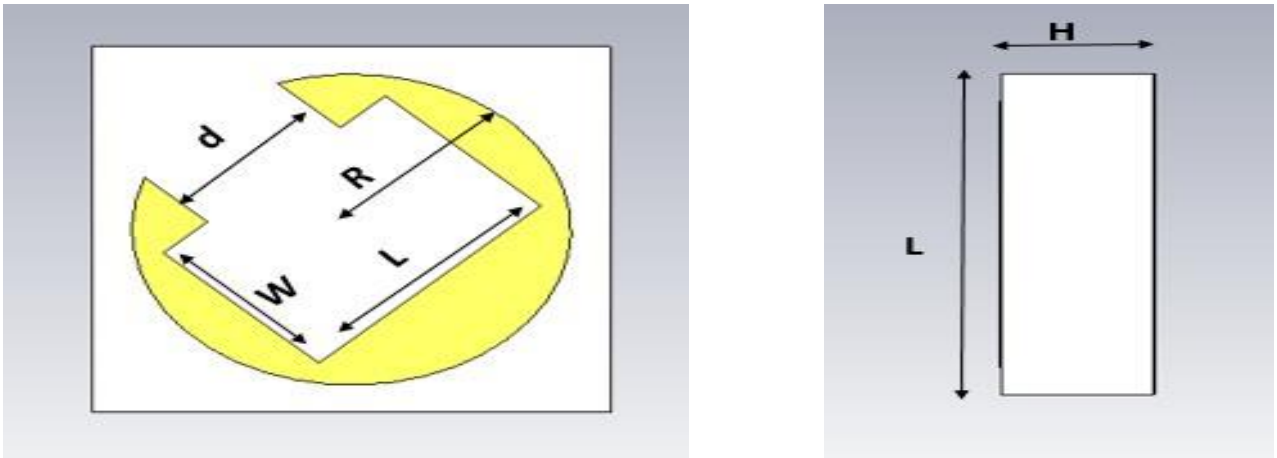

(a) (b)

Figure 3: (a) Front view of unit cell of reference MS (b) Side view of unit cell of reference MS.

To accurately simulate and analyze the proposed metasurface, appropriate material and geometric parameters were selected based on standard microwave design practices. FR4 was used as the substrate due to its suitable dielectric properties, and copper was chosen for the conducting parts owing to its high conductivity. The unit cell dimensions were optimized to ensure effective polarization conversion across the 4–20 GHz frequency range and the details of the parameters are summarized in Table 1.

Table 1: Reference MS Parameters

Parameters	Values (mm)
Substrate	FR4
Relative Permittivity	4.3
Loss tangent	0.025
Conductor Material	Copper
Copper Conductivity	5.8×10^7 s/m
Conductor Thickness	35µm
Opening gap (d)	3
Width (W)	3
Length (L)	5
Radius (R)	3.5
Height of substrate (h)	2.4
Periodicity (p) of unit cell	8.25
Frequency range	4GHz-20GHz

B. Unit Cell Design

The proposed metasurface works in reflection mode and comprises a two- dimensional periodic arrangement of C-shaped unit cell structure, as shown in Figure 3. The unit cell is modeled on the top of the FR4 dielectric substrate backed by a ground plane. The relative permittivity of the substrate is 4.3 and the loss tangent is 0.025. The C-shaped unit cell and ground plane are made of copper with a conductivity of 5.8×10^7 S/m and thickness 35 μm. The lengths of the geometrical parameters of the unit cell as shown in the extract of Fig. 1 are d = 3 mm, R=3.5mm, L = 5 mm, and W = 3 mm. The height h of the substrate is 2.4 mm and periodicity p of the unit cell is 8.25 mm.

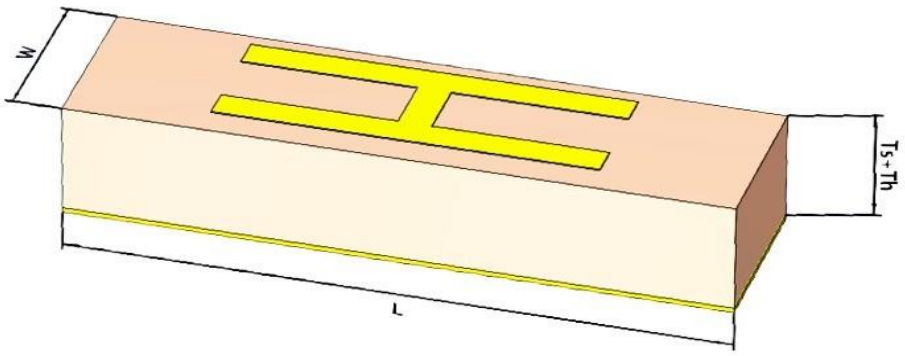

Figure 4: Unit cell of metasurface

C. Parametric Sweep Analysis:

optimal geometric configuration for achieving high-efficiency polarization conversion across multiple frequency bands. To optimize the metasurface for multifunctionality and broadband operation, a parametric sweep was conducted on the following key geometric parameters are provided given Table 2.

Table 2: Parametric Sweep analysis

Parameter	Range of Variation	purpose
Radius of the C-shaped (R)	2mm-4mm	Tune electrical length
Width of the C-arm (W)	2.5mm-4mm	Control magnetic coupling
Length of the resonator arm (L)	2mm-5mm	Adjust resonance position
Opening gap of he C-shape(D)	2mm-4mm	Control impedance matching and phase shift

D. Metasurface for Unit Cell

The proposed metasurface design is a reflective metasurface capable of beam steering at 300 GHz, which has significant importance for THz applications [29]. To obtain the appropriate reflection phases, the metasurface unit cell has an H-shaped structure. The unit cell design, shown in Figure 4, can reflect the incident wave. The parameters are provided in Table 3.

Table 3: Parameters for unit cell metasurface.

Parameters	values	description
L	300um	Length of unit cell
W	137.5um	Width of unit cell
Ts	100um	Thickness of substrate
Tg	4.5um	Thickness of ground
Th	1um	Thickness of H shape
Hw	25um	Arm width of H
Hd	50um	Gap between two arms of H
B	variable	Change from cell to cell in super cell

E. Design of Super cell

The actual design base on 16 unit cell which are combine to form super cell the super cell are design according to above parameter given in Table1 but having different arm length of H for each unit cell these arm length are 25.25um, 47.77um, 59.99um, 61.22um, 67.7um, 72.93um, 81.66um, 94.14um, 107.37um, 115.84um, 134.32um, 137.97um, 180.24um,258.39um, 288.41um, and 298 μm. The each dimension used in unit cell as well as super cell are in unit of micro. The complete supercell design is shown in Figure 5.

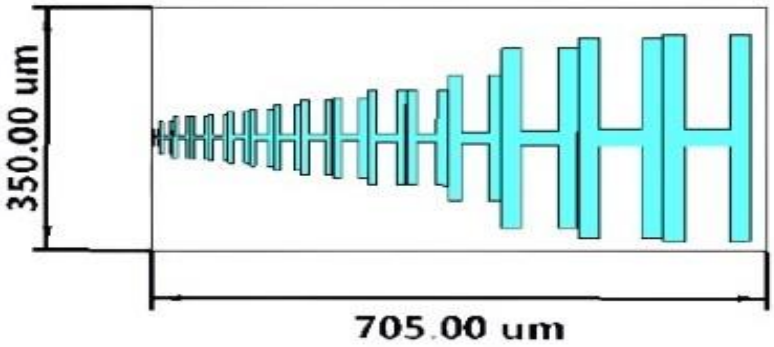

Figure 5: Schematic of complete super cell having 16 different arm's length

For super cell design 16 H shapes according to given values of B by using scale property of cst to adjust the size of H according to need place all H shapes in same work flow and use add command to add all 16 H shapes now design

F. First design of super cell:

The first design of the metasurface is shown in Figure 6. Hence, it is the same as discussed in Figure 5, with the only change being the substrate thickness, which is 100 µm

ground plane of same gold and then substrate of same thickness using transform property place and adjust the added H shaped structure on substrate.

.

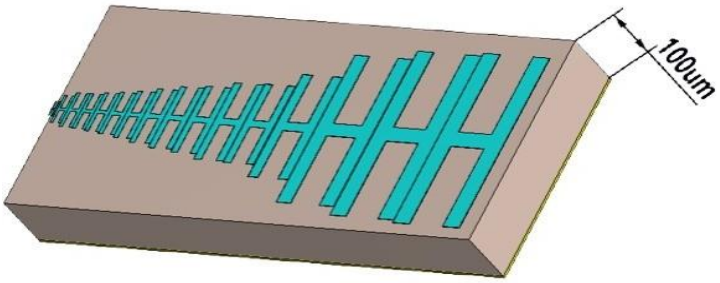

Figure 6: First design of super cell with substrate thickness 100um.

G. Second design of super cell:

The second design is shown in Figure 7. In thisdesign, we use the same method adopted for first design, but in this design, we increase the thickness of the substrate to 200 µm.

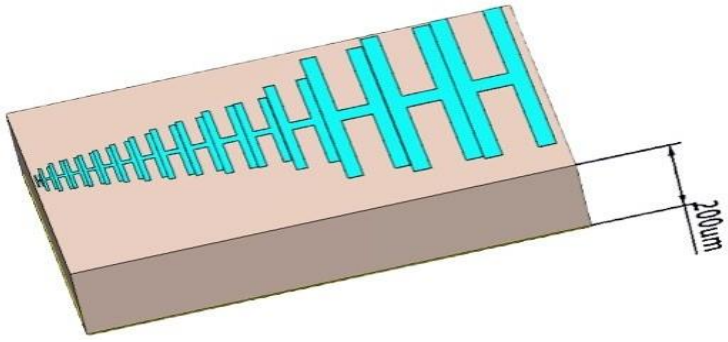

Figure 7: Second design of super cell with substrate thickness 200um

4. PROPOSED DESIGN & SIMULATION RESULTS FOR POLARIZATION CONVERSION

The simulation results of the proposed metasurface for polarization conversion were comprehensively analyzed to assess its effectiveness across the target frequency bands. The evaluation focused on the co-polarized and cross-polarized reflection coefficients, designated Ryy and Rxy, as well as the polarization conversion ratio (PCR). The criterion for efficient cross-polarization conversion required the co-polarized reflection component to remain below −10 dB, while the cross-polarized component should exceed −3 dB within the operating frequency ranges. As illustrated in Figure 8, the reference metasurface exhibited distinct resonant behavior at 5.35 GHz, 7.6 GHz, and 13.03 GHz, where the cross-polarized reflection was dominant and the co-polarized component remained suppressed. The simulation of x-polarized incidence produced similar results, as presented in Figure 9, demonstrating consistent performance for both orthogonal polarizations.

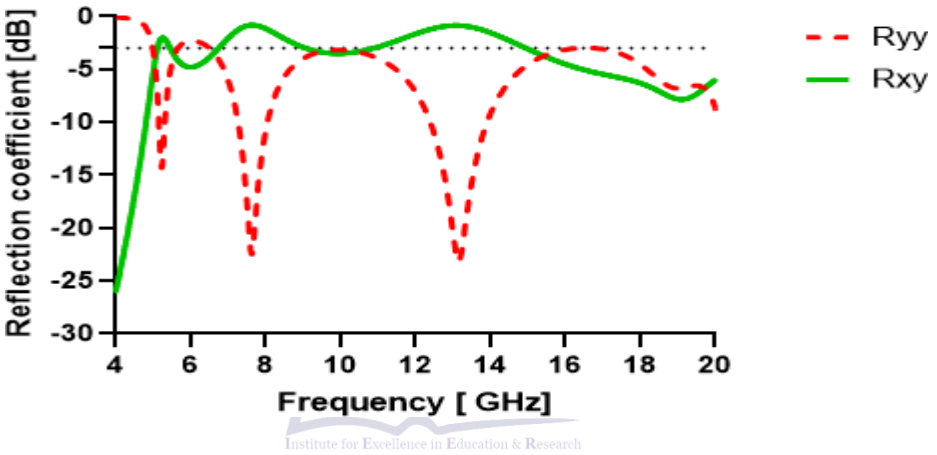

Figure 8: ***Ryy*** co-polarized reflection coefficient and the ***Rxy*** cross- polarized reflection coefficient with a frequency range from 4GHz to 20GHz.

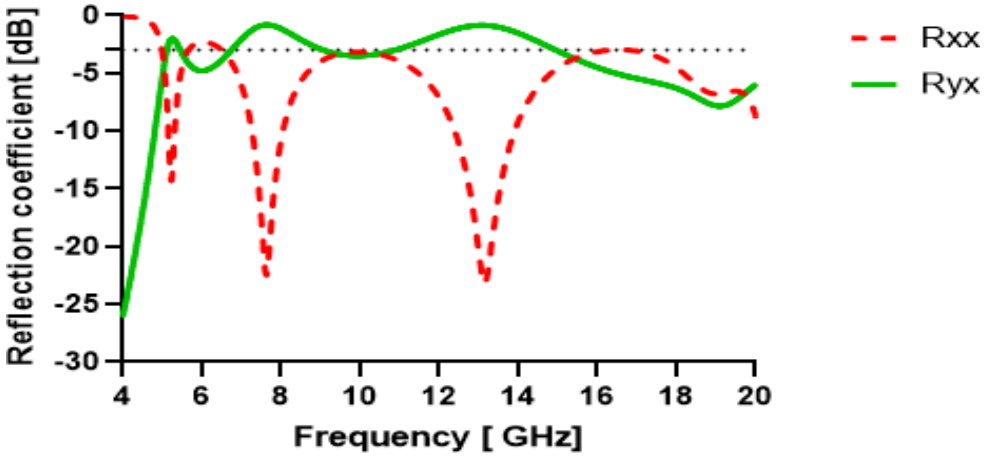

Figure 9: Rxx represents co-polarized reflection coefficient while Ryx represents the cross polarized reflection coefficient of x-poalrized.

The quantitative assessment of the PCR revealed that it exceeded 90% across the frequency intervals of 5.3–5.4 GHz, 7.2–8 GHz, and 12.3–13.76 GHz, while approaching nearly 100% at the strong resonances of 7.7 GHz and 13 GHz. The simulated PCR spectrum, shown in Figure 10, demonstrates that the metasurface maintains stable and efficient conversion within the desired bands. Further insight into the underlying mechanism of polarization conversion was obtained by analyzing the surface current distributions at the key resonance frequencies.

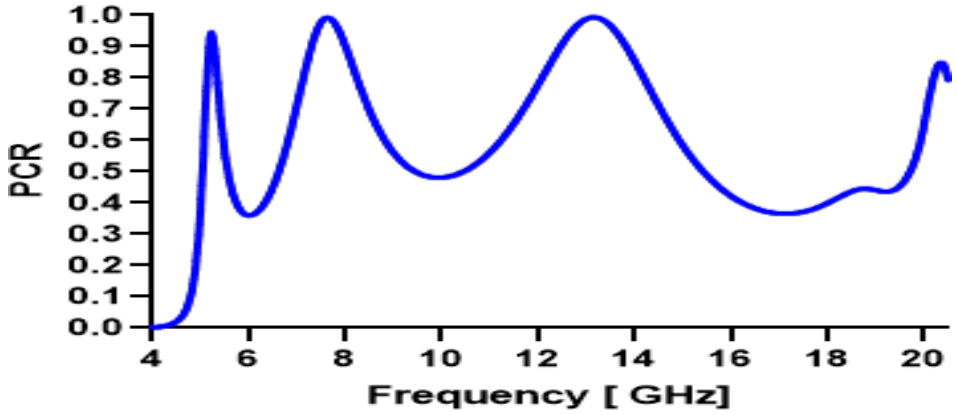

Figure 10: Polarization Conversion Ratio of Reference MS

To further optimize the polarization performance, a parametric sweep analysis was conducted by systematically varying four geometrical parameters: the radius (R), width (W), length (L), and opening gap (d) of the C-shaped resonator. The impact of each parameter variation on the reflection coefficients and PCR was evaluated across the frequency range. The results of sweeping the radius are shown in Figures 11, 12, and 13, which demonstrate an effective shift of resonance bands and additional suppression of the co-polarized reflection component. Variation of the width parameter resulted in an upward shift of resonance frequencies, as illustrated in Figures 14 and 15, while also improving the PCR levels.

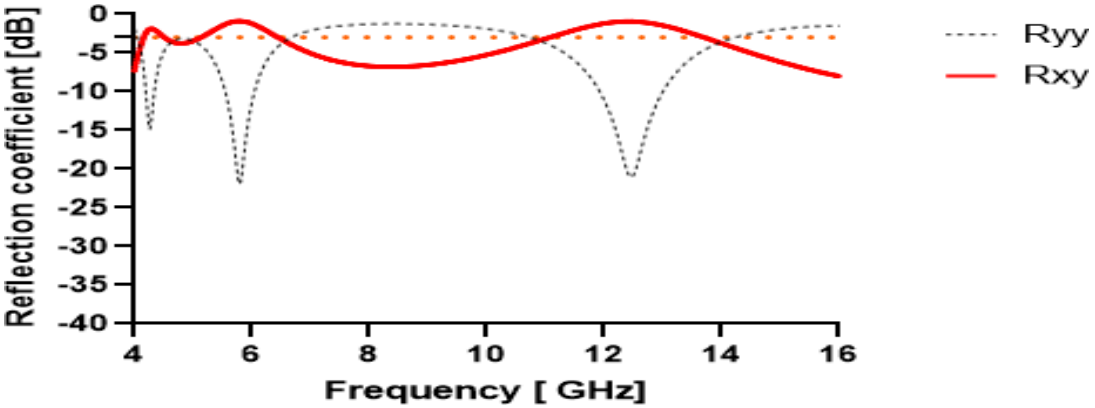

Figure 11: ***Ryy*** co-polarized reflection coefficient and the ***Rxy*** cross- polarized reflection coefficient with a frequency range from 4 GHz to 16 GHz.

Adjusting the length parameter contributed to enhanced polarization conversion near 13 GHz, as evidenced in Figures 16 and 17. Finally, modifying the opening gap improved impedance matching and yielded broader operational bandwidths, as shown in Figure 18.

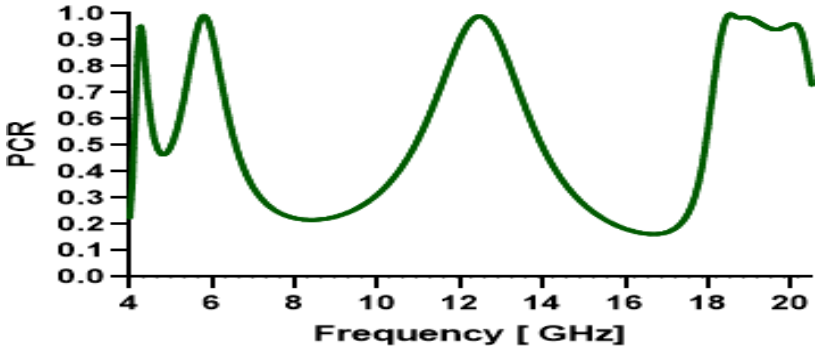

Figure 12: Effect on PCR by varying Parameter Radius (R)

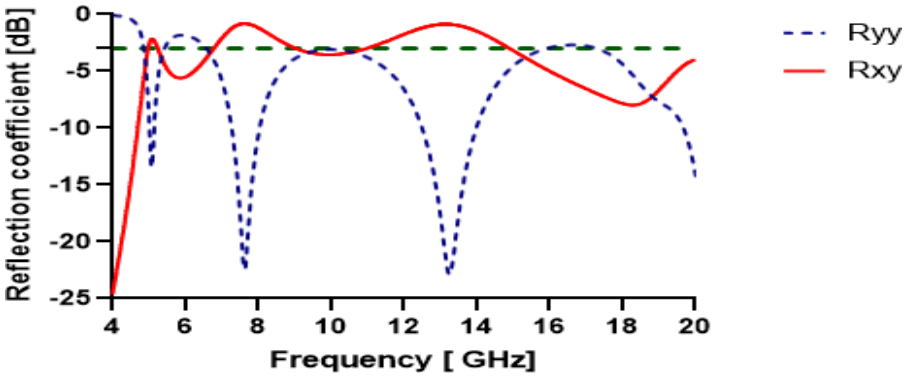

Figure 13: ***Ryy*** co-polarized reflection coefficient the***Rxy*** cross-polarized reflection coefficient with a frequency range from 4GHz to 20GHz.

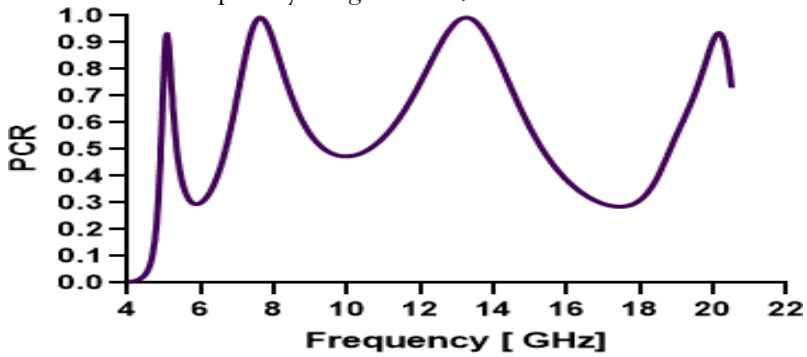

Figure 14: Effect on PCR by varying Parameter width (W)

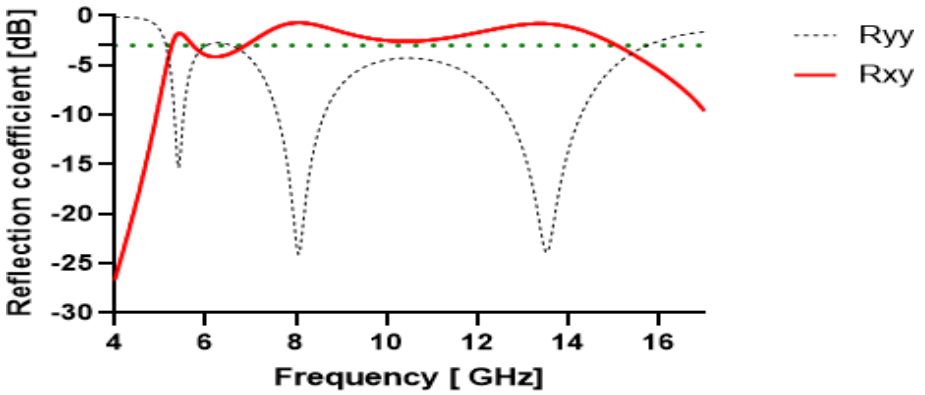

Figure 15: R_{yy} co-polarized reflection coefficient and the R_{xy} cross- polarized reflection coefficient with a frequency range from 4GHz to 20GHz.

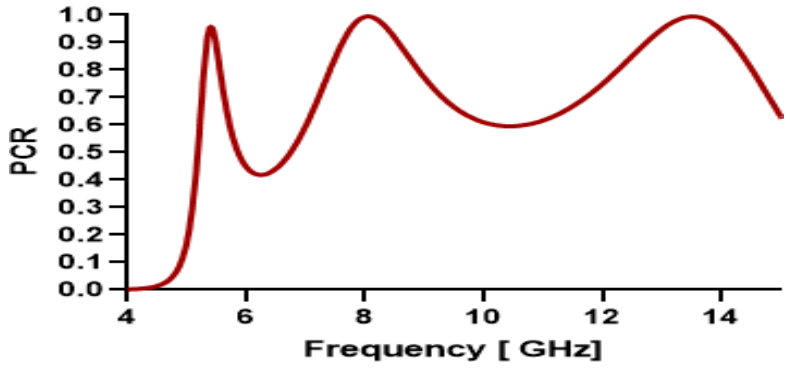

Figure 16: Effect on PCR by varying Parameter length (L)

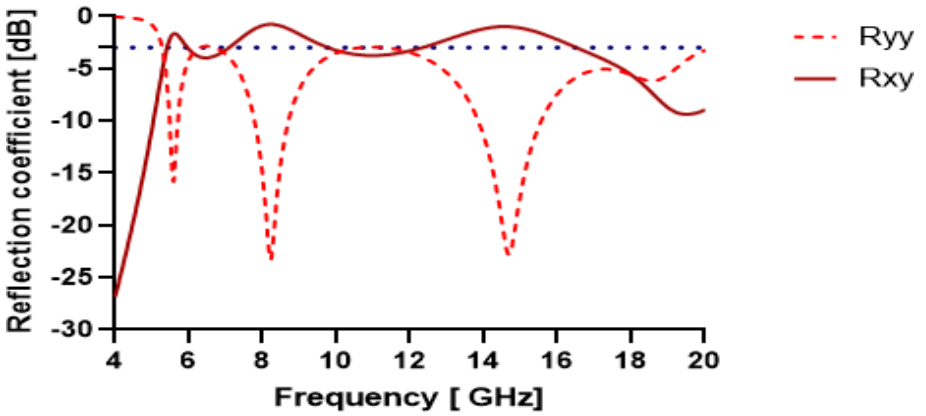

Figure 17: R_{yy} co-polarized reflection coefficient and the R_{xy} cross- polarized reflection coefficient with a frequency range from 4GHz to 20GHz.

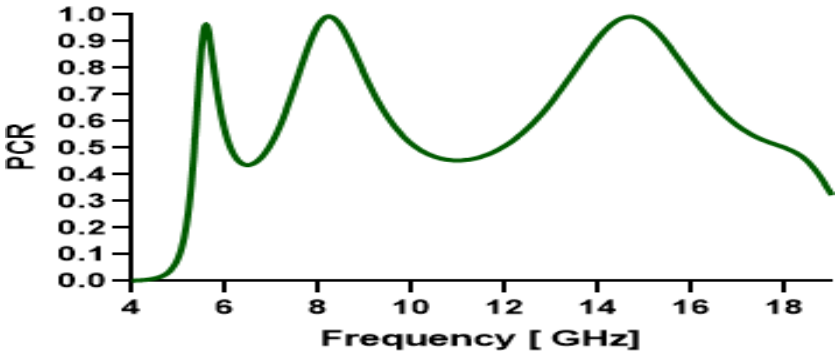

Figure18: Effect on PCR by varying Parameter opening gap (d)

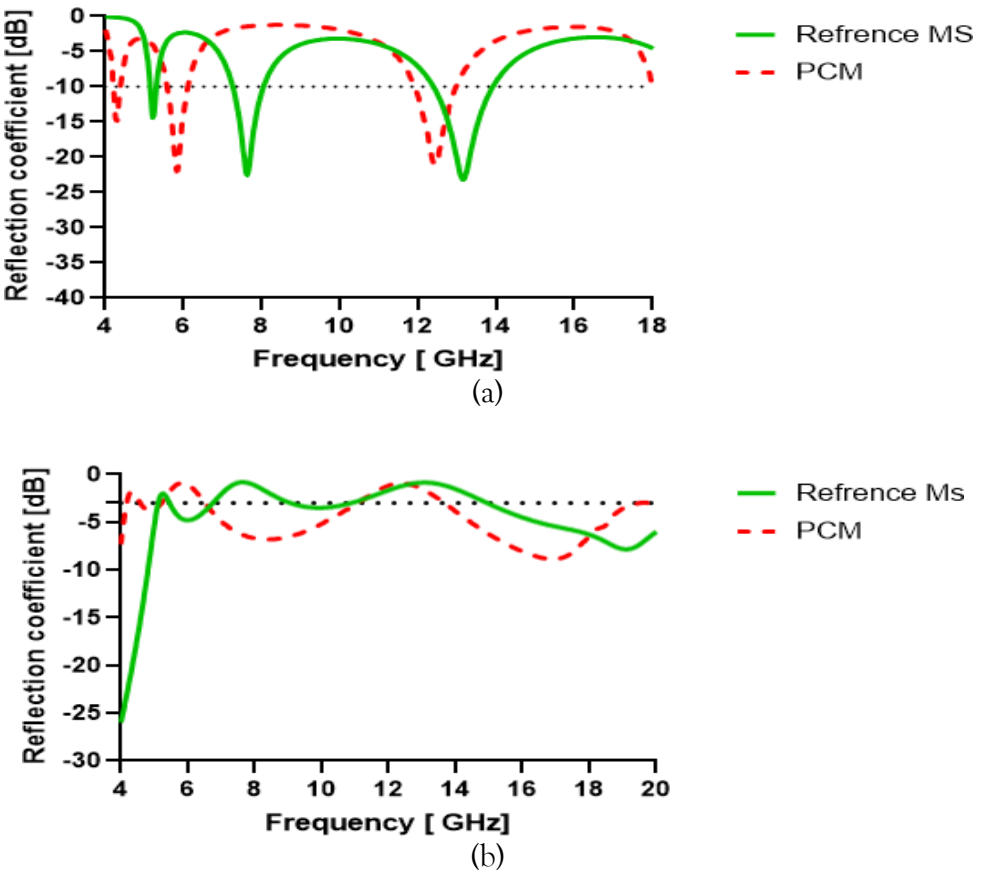

Figure 19: (a) Ryy co-polarized reflection coefficient (b) Rxy cross polarized reflection coefficient.

Comparative analyses between the optimized designs and the reference metasurface confirmed that the parametric adjustments led to consistent improvements in performance. The comparison of reflection coefficients and PCR for each parameter variation is presented in Figures 19(a) and 19(b), 20, 21(a) and 21(b), 22, 23(a) and 23(b), 24, 25(a) and 25(b), and 26, which

collectively illustrate the significant enhancement achieved by the proposed optimization strategy. These results validate the effectiveness of the metasurface design and highlight its capability to maintain high polarization conversion efficiency across multiple frequency bands, confirming its suitability for advanced applications.

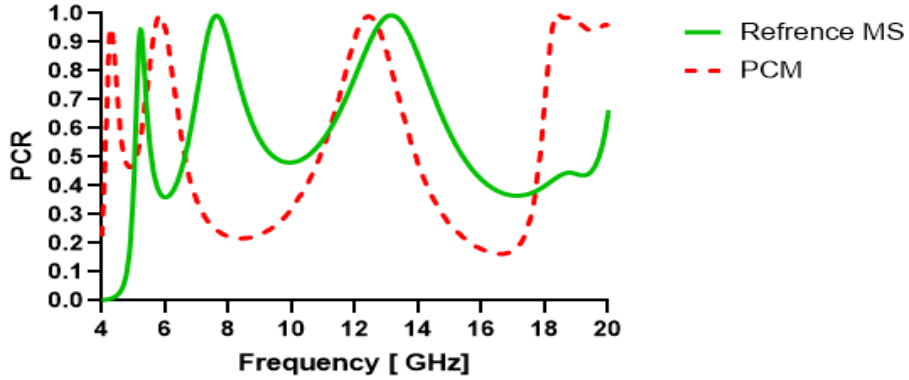

Figure 20: Comparing PCR by varying radius (R)

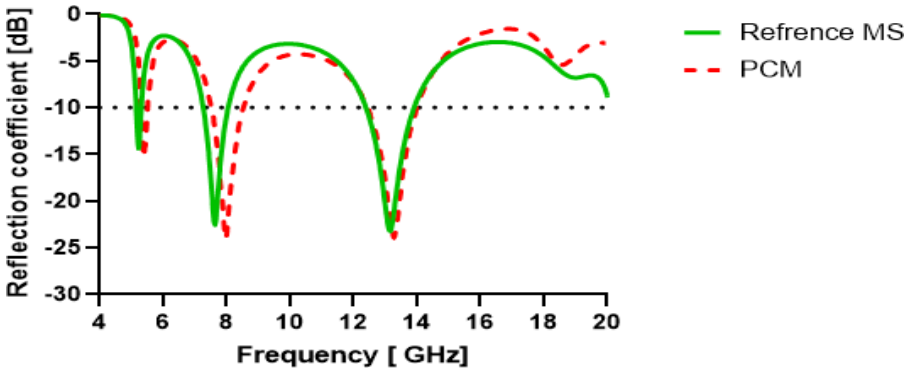

(a)

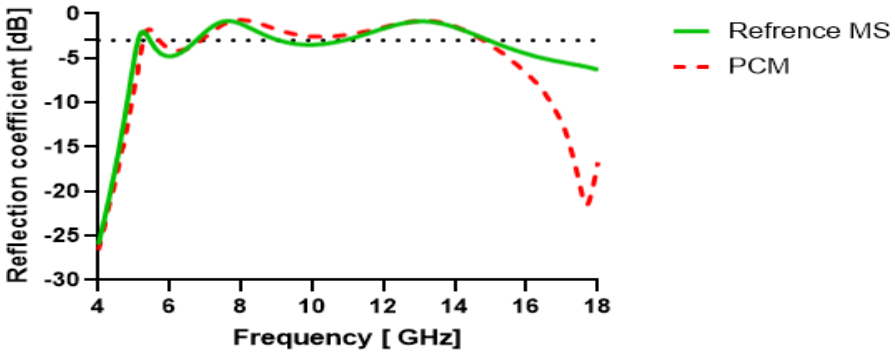

(b)

Figure 21: (a) Ryy co-polarized reflection coefficient (b) Rxy cross polarized reflection coefficient.

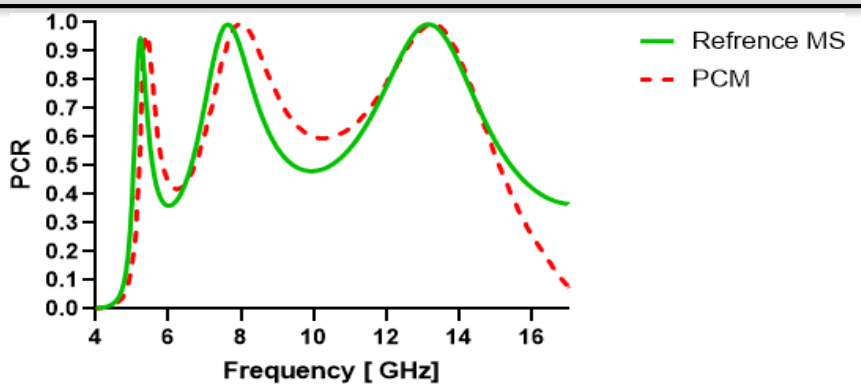

Figure 22: Comparing PCR by varying parameter length (L).

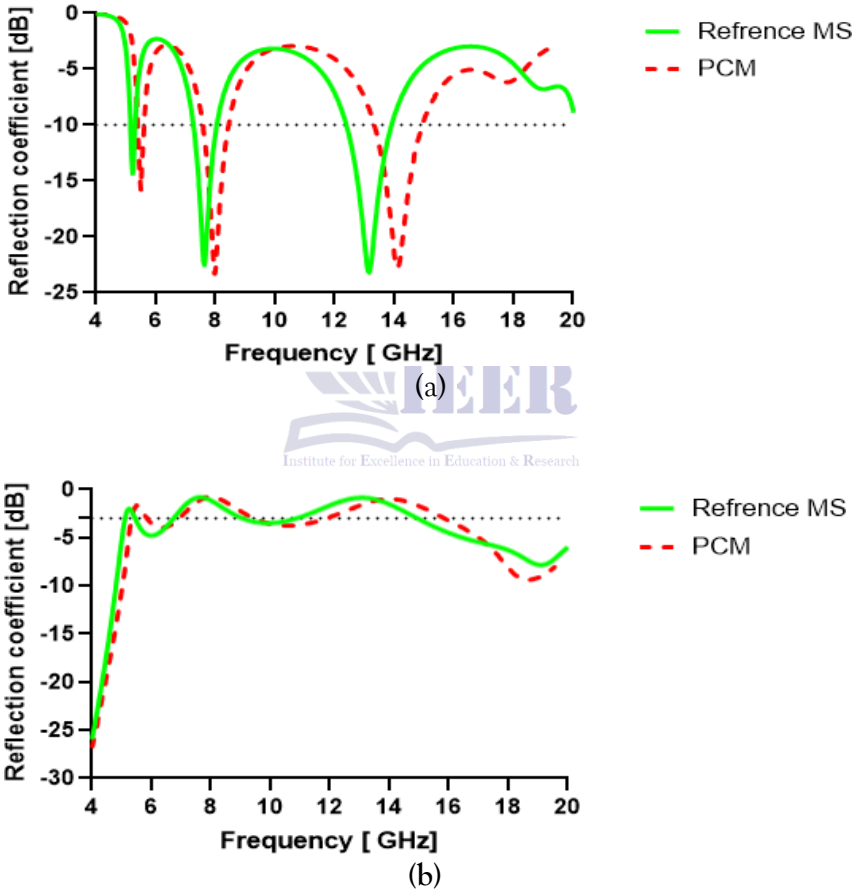

Figure 23: (a) Ryy co-polarized reflection coefficient (b) Rxy cross polarized reflection coefficient.

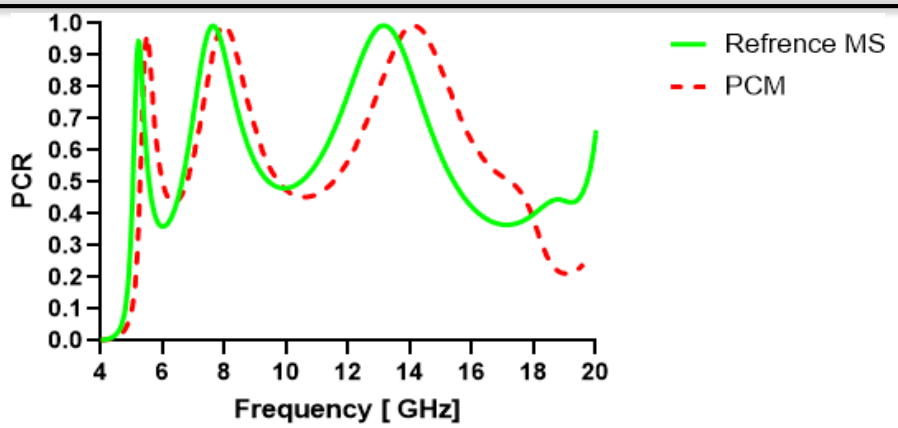

Figure 24: Comparing PCR by varying opening gap (d)

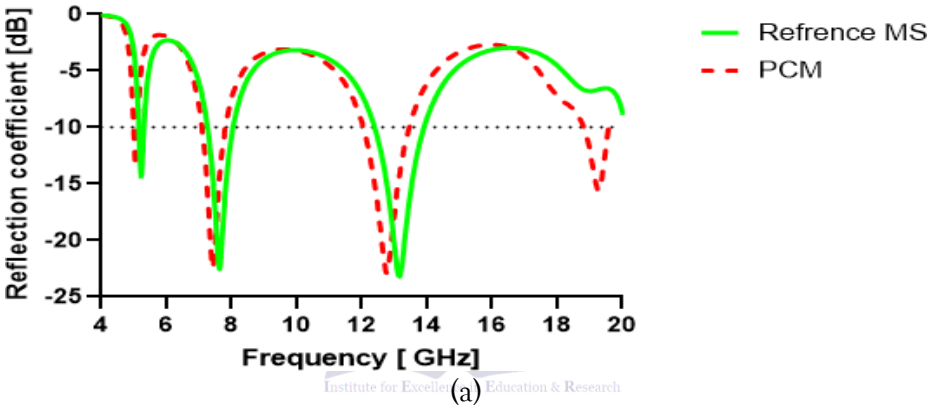

(a)

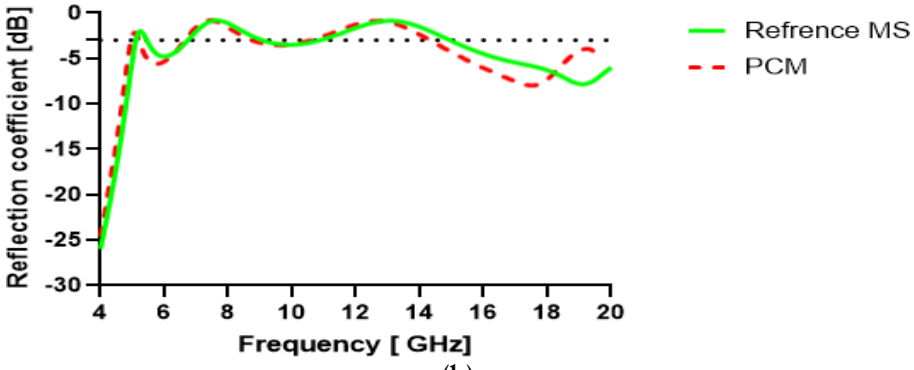

(b)

Figure 25: (a) Ryy co-polarized reflection coefficient (b) Rxy cross polarized reflection coefficient

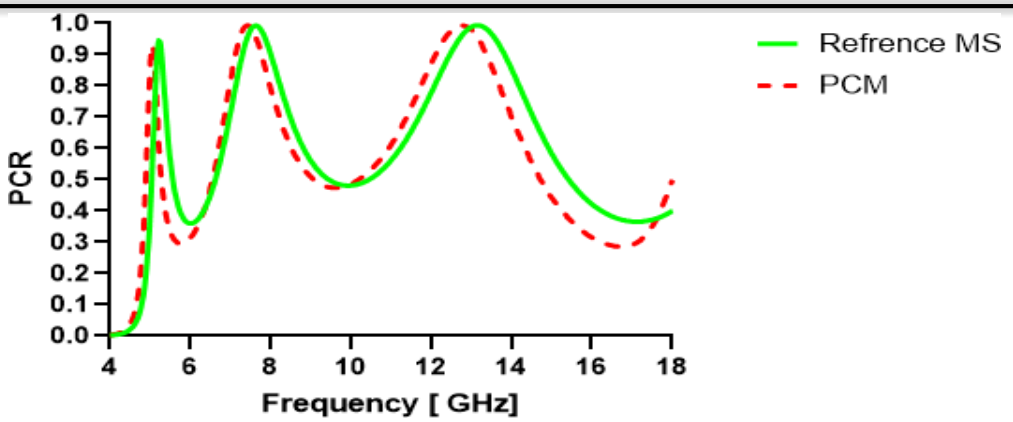

Figure 26: Comparing PCR by varying parameter width (W)

5. SIMULATION RESULTS FOR BEAM STEERING METASURFACE

To measure directionality and side-lobe behavior, this Study also assesses bistatic radar cross-section (RCS) patterns. In THz applications, the results strike a balance between phase control and reflection efficiency, supporting both static and dynamically configurable metasurfaces. The frequency range from 90 GHz to 300 GHz is considered for simulations.

The S11 parameter indicates how efficiently this metasurface unit cell reflects the incident wave, as shown in Figure 27. As the frequency rises from 90 GHz to 300 GHz, the phase shifts from +30° to approximately -850 °.According to this, metasurface provides 360° phase coverage and more, which is excellent for managing the reflection phase. When developing gradient metasurfaces for beam steering, the reflection phase must decrease gradually and monotonically. The proposed metasurfaces reflection phase response was assessed in a broad frequency range, from 90 GHz to 300 GHz. The reflection phase (S11 phase) exhibits a constant and almost linear change from +30° to 850°, as illustrated in Figure 27. This encompasses more than 870 degrees, which is equivalent to more than two complete phase cycles of 360 degrees. The meta materials' capacity to allow full 360° phase modulation is indicated by their wideband phase tenability, which is essential for beam steering and wavefront shaping.

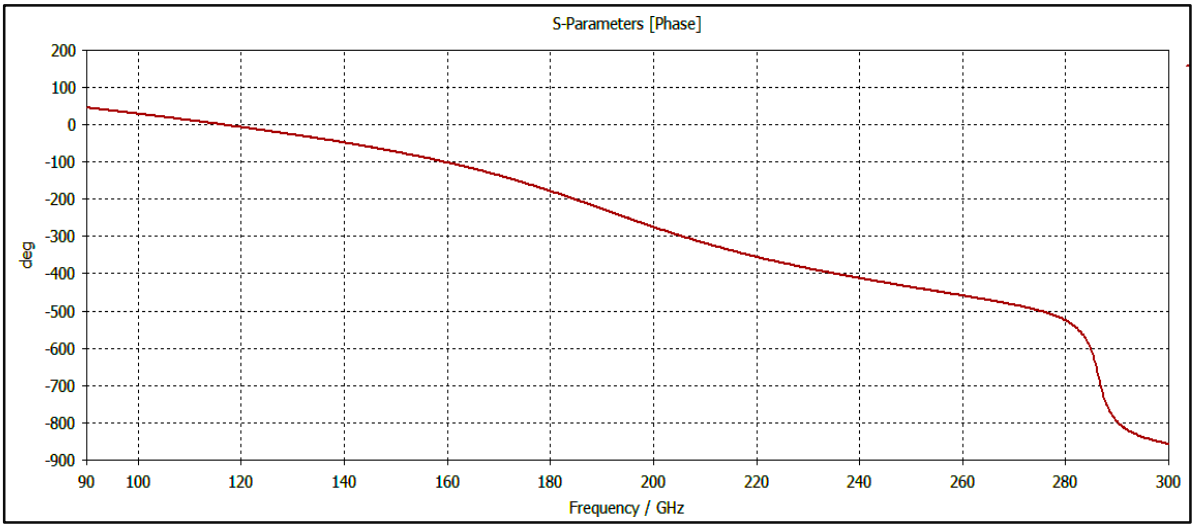

Figure 27: Reflection phase response as a function of b1 at 300 GHz

The bistatic RCS result has ability to show how metasurface can scatter the incident wave it is our main goal to show how our reflective metasurface can efficiently reflect the incident beam for getting RCS plot as shown in Figure 28. we perform simulation on one complete super cell having 16 different length of H shaped.

A. Result of First design of Metasurface

In the first design of the metasurface, we simulate and analyze the metasurface with a substrate thickness of 100 μm to investigate its behavior in response to the incident wave.

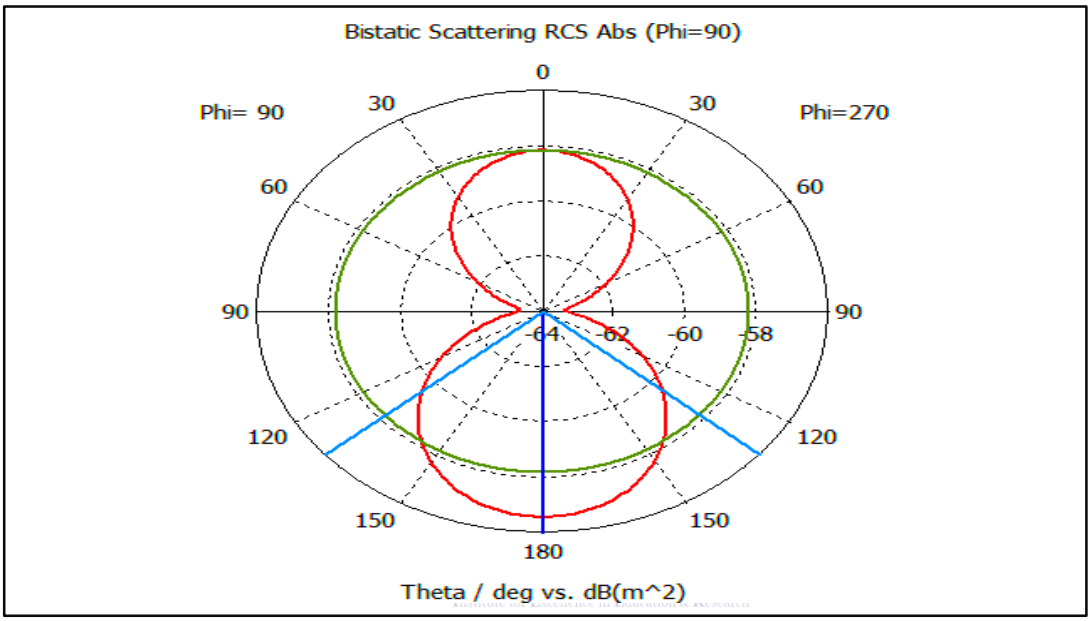

Figure 28: Simulated far-field radiation pattern of substrate thickness 100um.

Figure 28 shows the Plotting of the metasurface bistatic radar cross section (RCS) in polar coordinates as a function of the scattering angle θ at φ = 90°. The pattern shows suppressed scattering at side angles (θ = 90°, 270°) and prominent lobes in the forward (θ = 180°) and backward (θ = 0°) directions. Hence, it suggests that, due to its reflective design, the metasurface exhibits directional reflection behavior, focusing on the scattered energy along the plane of incidence. Its beam steering can be observed at certain angles by using a horn antenna. Applications involving wavefront control, such as beam redirection and RCS modulation, require this behavior.

B. Result of Second design of metasurface:

We change the thickness of substrate from 100um to 200um and observe some results which have their own benefits and also we make comparison between both results the simulation result of super cell metasurface having substrate 200um.

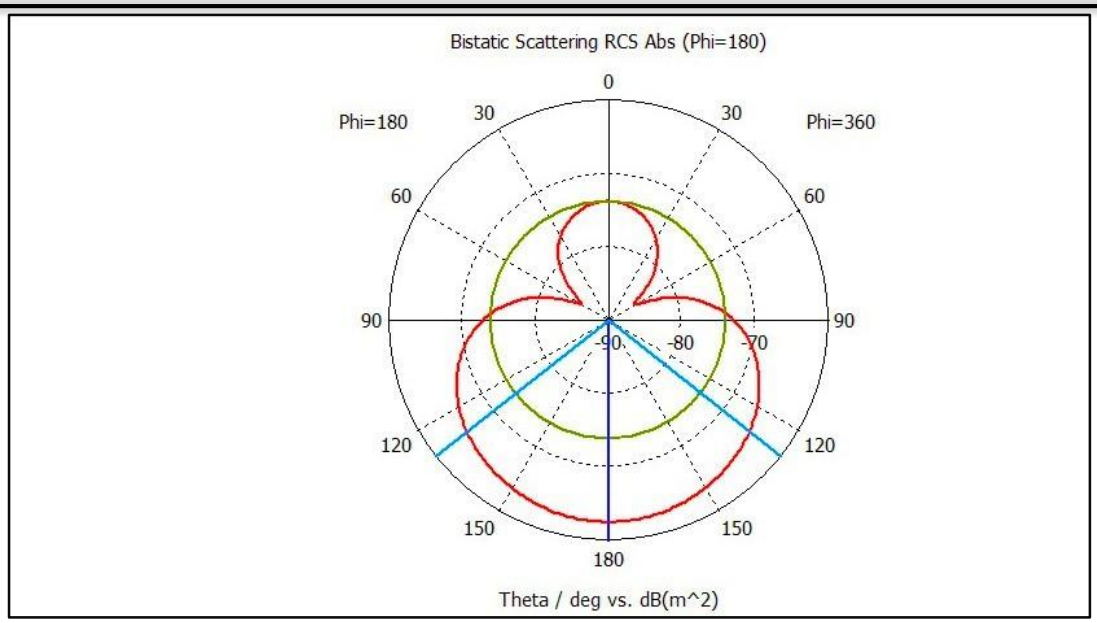

Figure 29: Radiation pattern of substrate thickness 200um

Figure 29 shows the bistatic radar cross-section (RCS) at Φ = 180°. The bistatic RCS result demonstrates a highly effective and directed reflection from the metasurface. Specular reflection, which indicates the structure's ability to reflect energy in the direction of the incident, is indicated by the presence of a strong main lobe centered at θ = 180°. The symmetrical pattern and smaller side lobes indicate that the metasurface is well-suited for directional backscattering, which is advantageous for wireless communication, radar, and sensing applications. The design is suitable for use in intelligent reflecting surfaces (IRS), retro-reflectors, and RCS shaping platforms, as the larger substrate size further enhances the coverage area and reflection strength. In high-frequency electromagnetic systems, the total performance shows that this metasurface design is both practically applicable and functionally efficient.

6. COMPARISON BETWEEN RCS OF SUBSTRATE SIZE 100UM AND 200UM

The comparison between the radar cross-section (RCS) performance of the metasurface designs with substrate thicknesses of 100 µm and 200 µm demonstrates distinct advantages and trade-offs associated with each configuration. The effectiveness of a reflective metasurface fundamentally depends on achieving a balance between phase control capability—the flexibility to adjust the phase of reflected waves—and reflection strength, which determines the capacity to scatter or redirect incident energy. In terms of main lobe magnitude, the design incorporating the 100 µm substrate exhibited a simulated main lobe level of −56.6 dB/m² for a single supercell. In contrast, the design with the 200 µm substrate achieved a main lobe level of −62.5 dB/m². These results indicate that the thinner substrate design exhibits stronger reflective behavior due to its higher primary lobe amplitude, resulting in enhanced scattering and improved radar detectability. Conversely, the lower main lobe of the thicker substrate suggests weaker scattering, which may be advantageous in

applications requiring reduced detectability, such as military or stealth technologies.

Regarding the 3 dB beamwidth, which defines the angular spread of the primary radiation pattern and correlates with the coverage area, the 100 µm substrate design demonstrated a beamwidth of 71.7 degrees, implying higher directivity and a more extended range, but a narrower coverage zone. In contrast, the 200 µm substrate yielded a beamwidth of 103.9 degrees, reflecting lower directivity but broader coverage, making it more suitable for omnidirectional or wide-area applications. Finally, analysis of side lobe levels, representing undesired energy radiated away from the main beam, revealed that the design with the 100 µm substrate had side lobes measured at −1.6 dB. In contrast, the 200 µm substrate design achieved substantially better suppression with side lobes at −11.3 dB. This lower side lobe level in the thicker substrate configuration indicates a greater ability to minimize interference and improve angular selectivity, which is essential in scenarios requiring precise directional performance. The comparison of RCS characteristics for the substrate in terms of thickness is provided in Table 4.

Table 4: Comparison of RCS Characteristics for Substrate Thicknesses 100 µm and 200 µm

Parameter	First Design (100 µm Substrate)	Second Design (200 µm Substrate)
Main Lobe Level	−56.6 dB/m²	−62.5 dB/m²
Interpretation	Higher reflectivity (stronger scattering)	Lower reflectivity (weaker scattering)

7. CONCLUSION

The present investigation outlines the design and optimization of a multifunctional metasurface antenna for effective polarization conversion and beam steering across a wide frequency range. The metasurface, employing a C-shaped unit cell, was simulated using CST Microwave Studio and exhibited remarkable polarization conversion ratios (PCR) over 90% throughout C-, X-, Ku-, and K-bands. Parametric analyses of geometric factors demonstrate enhanced bandwidth and conversion efficiency. The metasurface's twin capabilities, encompassing beam steering and polarization conversion, render it appropriate for satellite communication, 5G, and radar system applications. Performance assessments using the reflection phase and bistatic radar cross-section (RCS) simulations validate its wavefront modification capabilities. Future endeavors will focus on incorporating active components for real-time reconfigurability and enhancing beam steering efficacy for high-precision applications in radar, imaging, and terahertz communications.

REFERENCES

[1] T.-H. Lee, K.-J. Lee, W. Lim, and S.-H. Yi, "Exploring CP array antenna characteristics and its applications to a deployable structure," Sensors, vol. 25, no. 9, p. 2782, 2025.

[2] S. P. Gopi, S. Pathan, and J. Anguera, "A low-profile circularly polarized millimeter-wave broadband antenna analyzed with a link budget for IoT applications in an indoor scenario," Sensors, vol. 24, no. 5, p. 1569, 2024.

[3] M. Guo, P. Xin, H. Sun, H. Li, L. F. Chernogor, Z. Jin, and Y. Zheng, "Beam-steering flexible transparent metasurfaces based on multi-bit phase-gradient variations," Scientific Reports, vol. 15, p. 15467, 2025.

[4] C. Qian, L. Tian, and H. Chen, "Progress on intelligent metasurfaces for signal relay, transmitter, and processor," Light: Science & Applications, vol. 14, p. 93, 2025.
[5] L. Zhang, C. Gao, H. Guo, H. Zhang, and Z. Zhao, "Efficient polarization-conversion metasurface for scattered-beam control and RCS reduction," Scientific Reports, vol. 14, p. 26260, 2024.
[6] J. Zafar, H. Z. Khan, A. Jabbar, J. U. R. Kazim, M. U. Rehman, A. M. Siddiqui, and M. A. Imran, "Multi-band reflective metasurface for efficient linear and circular polarization conversion," Optical and Quantum Electronics, vol. 57, p. 149, 2025.
[7] J. Seong, Y. Jeon, Y. Yang, T. Badloe, and J. Rho, "Cost-effective and environmentally friendly mass manufacturing of optical metasurfaces towards practical applications and commercialization," International Journal of Precision Engineering and Manufacturing-Green Technology, vol. 11, pp. 685–706, 2024.
[8] S. Ali, F. Rahman, and J. Kim, "Design and measurement of a two-dimensional beam-steerable metasurface for Ka-band communication systems," Electronics, vol. 13, no. 10, p. 1998, 2024.
[9] X. Liu, W. Chen, Y. Zhang, and J. Yang, "Design of a 2.5-bit programmable metasurface unit cell for electromagnetic manipulation," Electronics, vol. 13, no. 9, p. 1648, 2024.
[10] S. Zhang, Q. Qin, and M. Hua, "A wideband polarization-insensitive bistatic radar cross-section reduction design based on hybrid spherical phase-chessboard metasurfaces," Coatings, vol. 14, no. 9, p. 1130, 2024.
[11] Y. Ma, Y. Ren, L. Wen, R. Zhao, K. Li, F. Wang, and H. Wu, "Dual-beam and dual circular-polarized multiplexing reflectarray for Ku-band satellite communication," Scientific Reports, vol. 15, p. 8772, 2025.
[12] B. M. Masini, C. M. Silva, and A. Balador, "The use of meta-surfaces in vehicular networks," Journal of Sensor and Actuator Networks, vol. 9, no. 1, p. 15, 2020.
[13] C. A. Balanis, Advanced Electromagnetics, Hoboken, NJ, USA: Wiley, 2012.
[14] S. A. Tretyakov, "Metasurfaces for general transformations of electromagnetic fields," Philos. Trans. R. Soc. A, vol. 373, no. 2049, Art. no. 20140362, 2015.
[15] M. Mencagli, E. Martini, and S. Maci, "MTS transformation for surface wave control," Philos. Trans. R. Soc. A, vol. 373, no. 2049, Art. no. 20140357, 2015.
[16] M. I. Khan, Q. Fraz, and F. A. Tahir, "Ultra-wideband cross polarization conversion metasurface insensitive to incidence angle," J. Appl. Phys., vol. 121, no. 4, p. 045103, 2017.